The Unfolded Protein Response Is Triggered by a Plant Viral Movement Protein[1][W][OA]

Changming Ye, Martin B. Dickman, Steven A. Whitham, Mark Payton, and Jeanmarie Verchot*

Department of Entomology and Plant Pathology (C.Y., J.V.) and Department of Statistics (M.P.), Oklahoma State University, Stillwater, Oklahoma 74078; Institute for Plant Genomics and Biotechnology, Department of Plant Pathology and Microbiology, Texas A&M University, College Station, Texas 77843 (M.B.D.); and Department of Plant Pathology, Iowa State University, Ames, Iowa 50011 (S.A.W.)

Infection with *Potato virus X* (PVX) in *Nicotiana benthamiana* plants leads to increased transcript levels of several stress-related host genes, including basic-region leucine zipper 60 (*bZIP60*), *SKP1*, ER luminal binding protein (*BiP*), protein disulfide isomerase (*PDI*), calreticulin (*CRT*), and calmodulin (*CAM*). *bZIP60* is a key transcription factor that responds to endoplasmic reticulum (ER) stress and induces the expression of ER-resident chaperones (*BiP*, *PDI*, *CRT*, and *CAM*). *SKP1* is a component of SCF (for SKP1-Cullin-F box protein) ubiquitin ligase complexes that target proteins for proteasomal degradation. Expression of PVX TGBp3 from a heterologous vector induces the same set of genes in *N. benthamiana* and Arabidopsis (*Arabidopsis thaliana*) leaves. Virus-induced gene silencing was employed to knock down the expression of *bZIP60* and *SKP1*, and the number of infection foci on inoculated leaves was reduced and systemic PVX accumulation was altered. Silencing *bZIP60* led to the suppression of *BiP* and *SKP1* transcript levels, suggesting that bZIP60 might be an upstream signal transducer. Overexpression of TGBp3 led to localized necrosis, but coexpression of TGBp3 with BiP abrogated necrosis, demonstrating that the unfolded protein response alleviates ER stress-related cell death. Steady-state levels of PVX replicase and TGBp2 (which reside in the ER) proteins were unaltered by the presence of TGBp3, suggesting that TGBp3 does not contribute to their turnover. Taken together, PVX TGBp3-induced ER stress leads to up-regulation of *bZIP60* and unfolded protein response-related gene expression, which may be important to regulate cellular cytotoxicity that could otherwise lead to cell death if viral proteins reach high levels in the ER.

Various cellular disturbances cause unfolded proteins to accumulate in the endoplasmic reticulum (ER), prompting a response that is conserved across kingdoms known as the unfolded protein response (UPR). External stimuli such as pathogen invasion, nutrient depletion, or Glc deprivation can exert stress on the ER by causing vigorous protein synthesis, aberrations in Ca^{2+} or redox regulation, inhibition of protein glycosylation, or protein transfer to the Golgi. These responses increase the levels of misfolded proteins in the ER and trigger the UPR. Export of malformed proteins from the ER into the cytosol is followed by degradation via the ubiquitin-proteasome pathway (Supplemental Fig. S1). Thus, the purpose of the UPR is to restore normal ER function, relieve stress exerted on the ER, and prevent the cytotoxic impact of malformed proteins (Jelitto-Van Dooren et al., 1999; Xu et al., 2005; Slepak et al., 2007; Urade, 2007; Preston et al., 2009).

Many UPR signaling components are conserved among mammals, yeast, and plants, although mammals and plants each have additional factors that lead to unique and complex sets of cellular responses (Xu et al., 2005; Zhang and Kaufman, 2006; Supplemental Fig. S1). Nutrient depletion or pharmacological agents, such as tunicamycin, have been used to map the plant signaling pathways relating to ER stress and the UPR (Williams and Lipkin, 2006). In both mammals and plants, the UPR mechanism involves increasing synthesis of several ER-resident proteins needed to restore proper protein folding, such as the ER luminal binding protein (*BiP*), protein disulfide isomerase (*PDI*), calreticulin (*CRT*), and calmodulin (*CAM*; Supplemental Fig. S1; Navazio et al., 2001; Ellgaard and Helenius, 2003; Oh et al., 2003; Urade, 2007; Seo et al., 2008). In tobacco (*Nicotiana tabacum*), *NtBLP-4* (the ER luminal binding protein *BiP*), *NtCRT*, and *NtPDI* were specifically up-regulated by ER stress-inducing compounds (Denecke et al., 1991, 1995; Iwata and Koizumi, 2005b). In fact, *NtBLP-4* is linked to prosurvival responses in plants and its overexpression alleviates ER stress (Leborgne-Castel et al., 1999). Other plant prosurvival factors include SDF2, which is a target of the UPR and contributes to plant development (Schott et al., 2010).

In homeostatic mammalian cells, BiP binds to ER-resident protein sensors such as IRE1, ATF6, and

[1] This work was supported by the U.S. Department of Agriculture National Research Initiative (project no. OKL02649) and Oklahoma Center for Advancement of Science and Technology Plant Biology Program (contract no. 7331).

* Corresponding author; e-mail verchot.lubicz@okstate.edu.

The author responsible for distribution of materials integral to the findings presented in this article in accordance with the policy described in the Instructions for Authors (www.plantphysiol.org) is: Jeanmarie Verchot (verchot.lubicz@okstate.edu).

[W] The online version of this article contains Web-only data.

[OA] Open Access articles can be viewed online without a subscription.

www.plantphysiol.org/cgi/doi/10.1104/pp.111.174110

PERK (Supplemental Fig. S1). However, during ER stress, BiP binds to misfolded proteins and releases its hold on these sensors. At the same time, IRE1, ATF6, and PERK respond to ER stress by inducing pathways that typically up-regulate cellular prosurvival signals but under extreme conditions can lead to prodeath signals. IRE1 and ATF6 represent sensors in the prosurvival pathways. In plants, *AtIRE1* and *AtBAG7* bind BiP and contribute to the maintenance of the UPR (Koizumi et al., 2001; Lu and Christopher, 2008; Williams et al., 2010).

Basic-region leucine zipper (bZIP) transcription factors are also fundamental contributors to the UPR (Supplemental Fig. S1). In mammals and yeast, the relevant bZIP transcription factors are XBP1, ATF6, and Hac1. In Arabidopsis (*Arabidopsis thaliana*), *bZIP60* is a membrane-bound transcription factor that is strongly induced following application of ER stress-inducing chemicals such as tunicamycin (Martínez and Chrispeels, 2003). *bZIP60* is activated by intramembrane proteolysis (Supplemental Fig. S1) and is translocated into the nucleus, where it up-regulates the expression of certain ER-resident chaperones such as *BiP*, *PDI*, and *CRT* (Iwata and Koizumi, 2005a; Urade, 2007; Iwata et al., 2008, 2009; Lu and Christopher, 2008). In tobacco, NtbZIP60 also localizes to the ER, responds to chemically induced ER stress, and is activated by nonhost bacterial pathogens (Tateda et al., 2008).

The SCF-type (for SKP1-Cullin-F box protein) E3 ubiquitin ligase complex (Murai-Takebe et al., 2004) contributes to the elimination of misfolded proteins in mammalian and plant cells via the 26S proteasome (Supplemental Fig. S1; Wang et al., 2006). However, little is known about protein recruitment for proteasomal degradation as part of the plant UPR. Der1-like proteins from maize (*Zea mays*) were reported to aid the degradation of misfolded proteins (Kirst et al., 2005). SKP1 is a highly conserved core protein in the SCF complex. The Arabidopsis and *Nicotiana benthamiana* SKP1 proteins participate in host defense to polerovirus infection (Pazhouhandeh et al., 2006), response to jasmonates during defense (Xu et al., 2002; Ren et al., 2005; Gfeller et al., 2010), and *Agrobacterium tumefaciens* tumorigenicity (Tzfira et al., 2004; Zaltsman et al., 2010). The role of ubiquitin ligase complexes in ER stress as well as in pathogen defense and susceptibility is particularly intriguing, since this study investigates the role of ER stress in virus infection. Without knowing a specific link between the UPR and the proteasome in plants, we chose to examine changes in *NbSKP1* expression following the application of a viral ER stress elicitor in an attempt to link virus-induced UPR with at least one component of the SCF complex.

Many mammalian RNA viruses manipulate host UPR signaling pathways to promote viral RNA translation and persistence in infected cells. These events are necessary to manage the increase in protein translation resulting from virus infection and membrane expansion needed for replication and maturation (Yu et al., 2006). For example, flaviviruses such as *Japanese encephalitis virus* (JEV) and dengue viruses (DEN) trigger the IRE1-XBP1 pathway, which leads to enhanced protein folding abilities, ER expansion, and up-regulation of the secretory system (Urano et al., 2000). While viral modification of the ER architecture has been explored in plants, there are no reported studies examining the role for UPR pathways in plant viral disease. Therefore, we decided to investigate whether *Potato virus X* (PVX) can also modulate UPR signaling pathways to modify the cellular environment, as described for many mammalian viruses. We explored the role of ER stress in PVX pathogenesis because of the broad range of viral proteins that are known to associate with the ER. For example, we recently reported that the PVX replicase (Rep) associates with the ER and that PVX infection is accompanied by expansion of the ER network (Bamunusinghe et al., 2009). The PVX TGBp2 and TGBp3 are low-molecular-mass proteins (12 and 8 kD) that also associate with the ER and contribute to cell-to-cell movement (Zamyatnin et al., 2002, 2006; Krishnamurthy et al., 2003; Mitra et al., 2003; Schepetilnikov et al., 2005). TGBp2 has two transmembrane domains, while TGBp3 has a single N-terminal transmembrane domain. ER association is necessary for these two proteins to promote virus spread, although the exact role of the ER in virus egress from the cell is not yet elucidated. Importantly, preliminary investigations indicate that TGBp2 and TGBp3 have distinct interactions with the ER network. When expressed in the absence of PVX infection, TGBp2 induces novel granular vesicles to bud from the ER (Ju et al., 2005). TGBp3, on the other hand, is distributed throughout the cortical ER network in membrane-bound subdomains alongside the viral Rep and is also packaged into TGBp2-containing granular vesicles (Samuels et al., 2007). These TGBp2-containing granular vesicles are required for virus cell-to-cell movement, although it is not known whether they function as containers carrying viral cargo to the periphery of the cell or play an alternative role in virus maturation and egress (Ju et al., 2005, 2007; Verchot-Lubicz et al., 2010).

Wild-type and aberrant forms of TGBp3 are exported from the ER and degraded by the 26S proteasome (Ju et al., 2005, 2008). Given the role of the proteasome in regulating viral protein accumulation and evidence that virus infection leads to expansion of the ER, we hypothesized that PVX infection could cause mild ER stress leading to up-regulation of the UPR. In this study, we provide evidence that PVX TGBp3 up-regulates UPR-related genes, including *bZIP60*, when it is expressed from the PVX genome or heterologous expression vectors. We investigate the role of ER stress in maintaining persistent virus infection and conclude that the UPR is a contributing factor toward promoting virus spread. We also link *bZIP60* to *SKP1* and UPR signaling and systemic accumulation of PVX.

RESULTS

Up-Regulation of the UPR during PVX Infection

We compared the gene expression profiles obtained using Arabidopsis and potato (*Solanum tuberosum*) microarrays, which were reported by Whitham et al. (2003) and García-Marcos et al. (2009), to identify common ER stress-regulated genes that are induced by PVX infection. In both investigations, UPR-related ER-resident chaperones such as *BiP*, *PDI*, and *CRT* were up-regulated, but only the potato microarray detected *CAM* (Supplemental Table S1). *bZIP60* and *SKP1* but not *IRE1* were predicted to be up-regulated in the published potato cDNA microarray probed with samples taken from PVX-infected *N. benthamiana* leaves (García-Marcos et al., 2009). Neither of the ER stress-related sensors *bZIP60* nor *IRE1* was represented on the Affymetrix Arabidopsis 8K GeneChip oligonucleotide microarray; therefore, their expression was not determined (Supplemental Table S1). The expression of *SKP1* was not reported to be altered in Arabidopsis, although it was represented on the microarray.

To further investigate gene expression associated with the UPR in PVX-infected leaves, quantitative reverse transcription (qRT)-PCR assessment of host transcript accumulation was performed using total RNA isolated from PVX-GFP-infected *N. benthamiana* leaves at 3 and 9 d post inoculation (dpi). Green fluorescent foci appear on the inoculated leaves at 3 dpi. The plants were fully and systemically infected at 9 dpi, although we extracted RNA from the inoculated leaves. Zero dpi represents samples that were harvested just before plants were inoculated with PVX-GFP. Given that the genome sequence for *N. benthamiana* is incompletely annotated, primers were designed for qRT-PCR based on the sequences of homologs from *N. tabacum* (*NtbZIP60*, *NtBLP-4*, *NtCAM*, *NtCRT*, and *NtPDI*) that have high homology to ESTs identified in the potato microarray (Supplemental Table S1).

Nonparametric analysis was used to describe the distribution of gene expression levels determined by qRT-PCR at 0, 3, or 9 dpi. This method of analysis provides excellent characterization of gene induction when using plant tissues that are not synchronously infected with PVX and/or if host gene expression is transiently altered (Bamunusinghe et al., 2009). Kruskal-Wallis tests (nonparametric ANOVA) were performed to assess the relationship of time to the various response variables. *P* values associated with the tests of equality of medians for each gene examined were less than 0.001, except for *CAM*, whose *P* value was 0.014. All *P* values indicate that PVX infection caused a significant increase in the expression of each gene over time.

PVX infection leads to a general increase in population values (representing fold changes in gene expression) for *bZIP60* (Fig. 1) at 3 and 9 dpi. The median values at 9 dpi are 3- to 4-fold higher, the border of the box representing the upper 75th percentile reaches 4- to 5-fold increase, and there is a maximum increase of 10-fold among outliers (Fig. 1; $P < 0.0001$). Such a general increase allows us to conclude that the gene is induced.

We can also conclude that a gene is induced based on the box-plot analysis, whereby values have a positively skewed distribution. The median values for *SKP1*, *BiP*, *PDI*, *CRT*, and *CAM* at 0 dpi were approximately 0.9, with the range of values extending from 0.05 to 2.3 (Fig. 1). The median values for *BiP* and *SKP1* increased to 3.4-fold at 9 dpi. The range of values for *BiP* and *SKP1* expression was positively skewed (represented by elongation of box and whiskers above the median) and showed elevated values of 5.6- and 7.5-fold, respectively, and maximum values of 8- and 10-fold (Fig. 1; $P < 0.001$).

PVX infection also leads to significant changes in *CRT* transcript accumulation, while *CAM* and *PDI* values show a mild positive change at 9 dpi. The boxes and whiskers for *PDI*, *CRT*, and *CAM* were generally small, indicating low dispersion of values among the plants analyzed. For *CAM*, *PDI*, and *CRT*, the median values at 9 dpi increased to approximately 1.7-, 2.0-, and 2.5-fold, respectively. *CRT* expression among plants in the 75th percentile showed up to 4.5-fold increase ($P = 0.007$), while for *CAM* and *PDI*, the value ranges were moderately changed (Fig. 1; PDI, $P < 0.01$; CAM, $P = 0.0143$). The increased expression of *bZIP60*, *BiP*, *CAM*, *PDI*, and *SKP1* clearly suggests that PVX infection coincides with the up-regulation of UPR.

TGBp3 Causes UPR-Related Gene Induction following Agrodelivery

To study the mechanism of UPR induction and identify the viral inducers, we employed *A. tumefaciens*-mediated transient expression in a reproducible and quantitative assay. The entire PVX genome and each PVX gene were expressed from a binary vector containing the cauliflower mosaic virus (CaMV) 35S promoter (Fig. 2A) for agrodelivery to *N. benthamiana* leaves. By comparing host gene expression following agrodelivery of each PVX gene, we could learn whether UPR induction is a general response to virus infection or is specifically induced by a single PVX factor. PVX encodes three proteins that associate with the ER (Rep, TGBp2, and TGBp3), and any or all of these could cause up-regulation of ER stress-related genes. Given that the UPR is often associated with ER stress, we predicted that one or more ER-resident factors would be responsible for host gene induction.

Initial immunoblot analysis was carried out to confirm PVX gene expression in *N. benthamiana* leaves following agrodelivery. Since we lack antisera detecting PVX Rep, TGBp2, or TGBp3, either a myc- or 6x-His tag was fused to these PVX genes (Fig. 2A) and immunoblot analysis was carried out using either anti-myc or penta-His antisera. We introduced the 6x-His tag into the PVX genome at the 3′ end of TGBp3

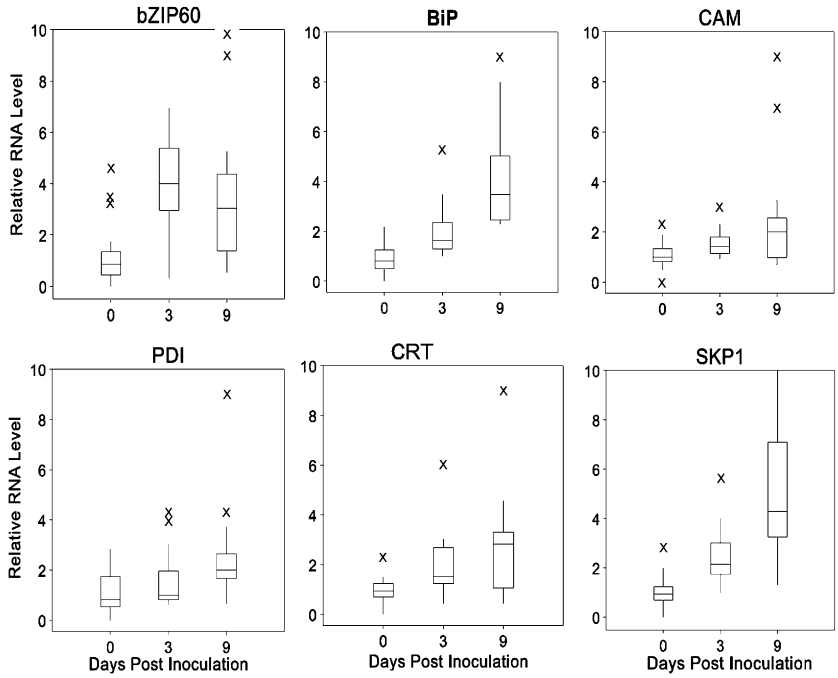

Figure 1. Box plots representing qRT-PCR analysis of transcript levels in PVX-infected *N. benthamiana* leaves. Genes are indicated above each graph. Box plots represent the range of values obtained for 20 samples and the variability of gene expression. The boundaries of each box represent the lower 25th and upper 75th percentiles, and the horizontal line within the box represents the median value (i.e. 50th percentile). The spacing of components within the box indicates the degree of dispersal, or skewness, in the data. The lines at the top and bottom of the box (whiskers) represent the sample minimum and maximum. Longer lines at the top indicate a positive skewness. Outliers are indicated by ×. Kruskal-Wallis test of the equality of medians reported *P* values as follows: for bZIP60, $P < 0.0001$; for BiP, $P < 0.001$; for PDI, $P = 0.007$; for CAM, $P = 0.0143$; for CRT, $P = 0.007$; and for SKP1, $P < 0.0001$.

without altering virus infectivity, but we were not able to make similar insertions to fuse myc tags to Rep or TGBp2. The 3′ end of Rep overlaps with the TGBp1 subgenomic promoter, and adding a tag here would destroy the function of the subgenomic promoter. Also, the TGBp2 promoter and coding sequence overlap with TGBp1 and TGBp3, and a fusion in the endogenous sequence would eliminate the functions of the overlapping genes. However, the N-terminal myc fusion was expected to be functional, because GFP-TGBp2 fusions facilitated PVX infection (Ju et al., 2005). Thus, immunoblot analysis in Figure 2B confirms Rep and TGBp2 expression from the CaMV 35S promoter but cannot compare the levels of expression of the same genes from the PVX genome. On the other hand, the levels of TGBp3, TGBp1, and coat protein (CP) are comparable when expressed from the PVX genome or directly from the CaMV 35S promoter (Fig. 2B).

N. benthamiana leaves were infiltrated with each binary construct, total RNA was extracted at 2 and 5 d post infiltration, and qRT-PCR was carried out. Controls include leaves infiltrated with buffer (mock) or *A. tumefaciens* alone. Since agroinfiltration results in synchronous delivery of PVX and each PVX gene to plant cells, the values obtained were less dispersed than in plants inoculated with purified virus.

Interestingly, TGBp3 delivery resulted in 3.5- to 4-fold higher levels of *BiP*, *bZIP60*, *CRT*, and *SKP1* transcript accumulation at 2 dpi in comparison with mock-inoculated plants. At 5 dpi, *BiP*, *bZIP60*, *CRT*, *CAM*, and *SKP1* showed 4- to 5-fold higher expression (Fig. 2C; $P < 0.05$). *PDI* induction was approximately 2-fold. Similarly, the expression levels of *bZIP60*, *BiP*, *CAM*, *PDI*, and *SKP1* in PVX-infected *N. benthamiana* leaves averaged 2- to 4-fold above the mock control at 2 d post infiltration (Fig. 2C; $P \leq 0.1$). Since the level of TGBp3 expression is comparable with the level of expression from the PVX genome, it is not likely that such high levels of *bZIP60*, *BiP*, *CAM*, *PDI*, and *SKP1*are due to cytotoxic overexpression of TGBp3 but are more likely due to a real effect of TGBp3 on the host. Since the level of gene induction during PVX infection is not as profound as TGBp3 alone, it is reasonable to consider that there might be other viral proteins interacting with TGBp3 during virus infection that may suppress the effect of TGBp3 on the host.

We also noticed 2-fold induction of *BiP* and *bZIP60* by Rep and CP at either 2 or 5 dpi. TGBp2 also induces SKP1, suggesting that its up-regulation may be independent of bZIP60-controlled pathways. The effects of these other PVX proteins are not as profound as TGBp3. Notably, *CRT* appears to be induced by PVX and several of its genes, suggesting that its induction is more likely the result of a generalized response.

UPR Induction in Arabidopsis

Given that the microarray data identified the same set of host factors induced in Arabidopsis and *N. benthamiana* plants, we employed the same TGBp3-containing binary vector to examine the ability of TGBp3 to induce UPR-related genes in Arabidopsis. Immunoblot analysis also confirmed successful expression of TGBp3His from the CaMV 35S promoter following agrodelivery to Arabidopsis leaves (Fig. 3A). For Arabidopsis, the average level of induction of *AtbZIP60*, *AtBiP2*, and *AtCAM2* was 2- to 5.5-fold at

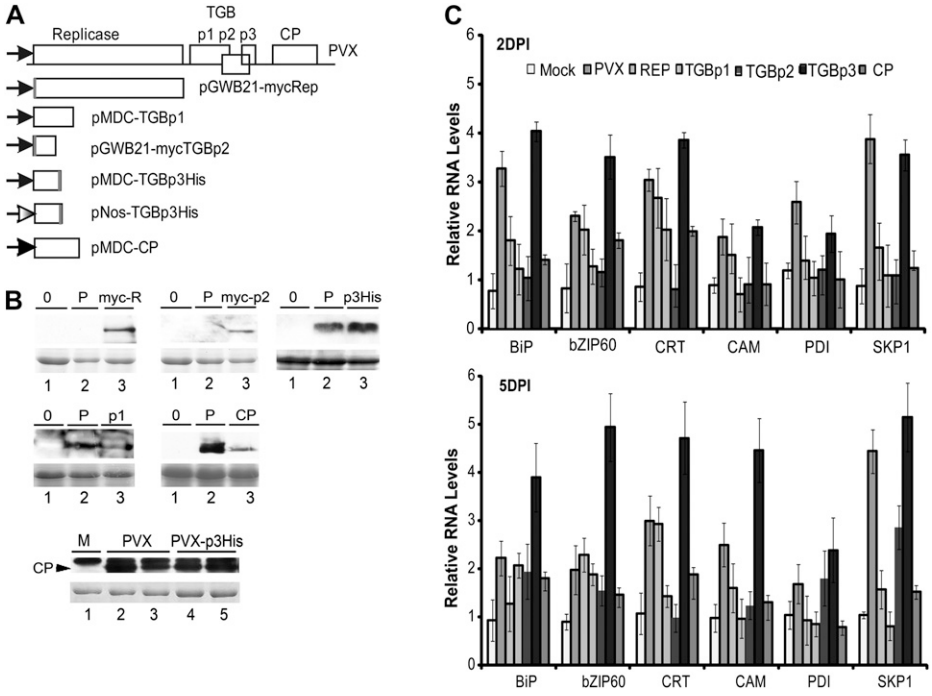

Figure 2. TGBp3 induction of BiP, CAM, CRT, PDI, SKP1, and bZIP60 transcripts following agroinfiltration. A, Diagrammatic representation of constructs used in this study. The black arrows indicate the CaMV 35S promoter, and the light gray arrow indicates the NOS promoter. The boxes represent open reading frames. The name for each construct is listed on the right. The gray bars indicate myc or His tags. B, Immunoblots containing protein extracts from *N. benthamiana* leaves that were infiltrated with buffer (0; lane 1) or *A. tumefaciens* containing PVX-GFP (P), mycRep (myc-R), mycTGBp2 (myc-p2), TGBp3His (p3His), TGBp1 (p1), and CP. The immunoblot at the bottom shows PVX-GFP and PVX-p3His. The latter contains a His tag fused to TGBp3, and immunoblotting was carried out using CP antisera. The immunoblot shows that CP levels are comparable in systemic tissues at 7 dpi, indicating that the His tag is not deleterious to virus accumulation. The antisera used for protein detection are identified below the blots. The PVX used in these experiments has the His tag fused to TGBp3; therefore, His antisera can detect TGBp3 in the PVX genome. C, Leaves were agroinfiltrated, total RNA was extracted at 2 or 5 dpi, and qRT-PCR was carried out. Values represent averages of three replicate samples.

2 and 5 d post infiltration, indicating that these are early and stable responses to the viral protein (Fig. 3A; $P < 0.05$). *AtCRT2* and *AtPDI2-1* were up-regulated at 5 d post infiltration (Fig. 3A; $P < 0.05$). *AtSKP1*, *AtCRT2*, and *AtPDI2* transcripts accumulated to significant levels, ranging from 2- to 5.5-fold above control samples at 5 d post infiltration (Fig. 3A; $P < 0.05$).

Induction Is Related to the Strength of the Promoter Driving TGBp3 Expression

We also examined whether gene induction in *N. benthamiana* is dependent upon the promoter driving expression or the concentration of *A. tumefaciens* infiltrated into the leaves. Leaves were infiltrated with *A. tumefaciens* carrying binary plasmids containing TGBp3 fused either to the NOS or CaMV 35S promoter. Protein expression was lower from the NOS promoter relative to the CaMV 35S promoter (Fig. 3B). Various dilutions of *A. tumefaciens* (optical density at 600 nm [OD_{600}] = 1.0, 0.1, or 0.01) were delivered to *N. benthamiana* leaves to determine if there is a dosage-dependent response. In general, host gene induction was greatest at 2 and 5 dpi, when 1.0 OD_{600} of *A. tumefaciens* solution was used, and induction was proportionally less with each dilution (Fig. 3B). The NOS promoter is weaker than the CaMV 35S promoter, and this led to somewhat lower fold changes in expression of UPR-related genes (Fig. 3B). Collectively, these data demonstrate that expression of TGBp3 alone is sufficient to induce the expression of UPR-related genes and that the TGBp3 levels correlate with the magnitude of induction.

Suppression of *bZIP60* and Its Impact on *BIP* and *SKP1* Expression

BiP is an ER-resident member of the Hsp70 family, and its expression is a marker for ER stress and the UPR. bZIP60 is known to up-regulate BiP as part of an ER stress response (Iwata and Koizumi, 2005a), but it is not the only transcription factor responsible for its up-regulation. SKP1 is a component of the SCF-type E3 ubiquitin ligase complex (Murai-Takebe et al., 2004) that is implicated in the elimination of misfolded proteins in mammalian and plant cells via the 26S

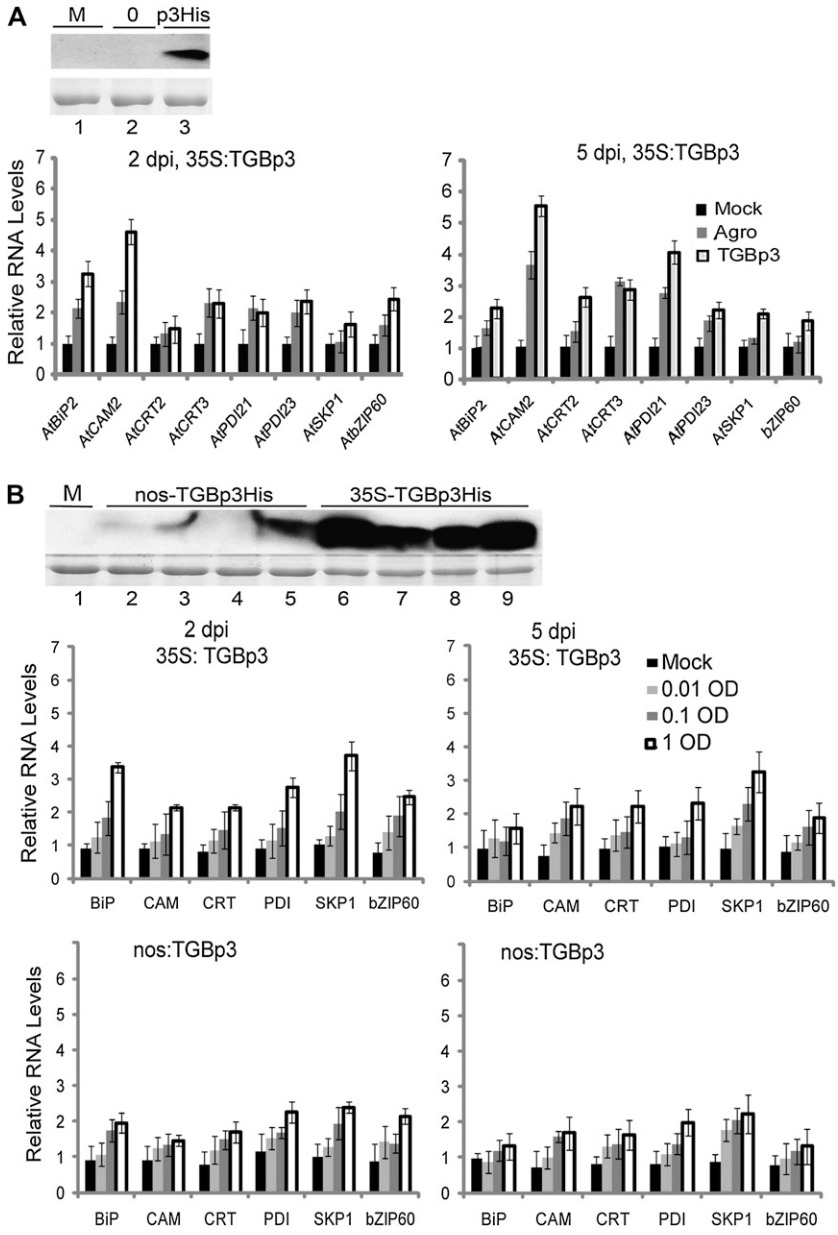

Figure 3. Induction following delivery of TGBp3 to Arabidopsis and using alternative ectopic promoters. The top of each panel shows an immunoblot probed with His antisera. In A, the immunoblot contains protein extracts from Arabidopsis leaves that were infiltrated with buffer (M), *A. tumefaciens* only (0), or *A. tumefaciens* containing plasmids expressing TGBp3-His. In B, the immunoblot contains protein extracts from *N. benthamiana* leaves that were infiltrated with *A. tumefaciens* containing TGBp3 fused to either the NOS promoter (lanes 2–5) or the CaMV 35S promoter (lanes 6–9). These immunoblots verify protein expression in planta. The Coomassie blue-stained gel located below each immunoblot shows equal sample loading on the gel. A, Arabidopsis leaves were infiltrated with buffer (mock), *A. tumefaciens* only (Agro), or *A. tumefaciens* expressing 35S-TGBp3. Total RNA was extracted at 2 or 5 dpi, and qRT-PCR was carried out. The average of three replicate samples is represented by each bar. ANOVA was used to verify that TGBp3 induced higher levels of host transcripts than other treatments at that time point ($P < 0.05$). B, *N. benthamiana* leaves were infiltrated with buffer (mock) or dilutions of *A. tumefaciens* containing TGBp3 fused to either the CaMV 35S or NOS promoter.

proteasome (Supplemental Fig. S1; Wang et al., 2006), and it is unknown whether bZIP60 might also be responsible for its up-regulation. Because *bZIP60*, *BiP*, and *SKP1* expression was induced by TGBp3, we hypothesized that *bZIP60* is an upstream transducer responsible for elevated levels of *BiP* and possibly *SKP1*. Importantly, Figure 2 also shows that there is a 2-fold induction of BiP by other PVX factors and approximately 3-fold induction of SKP1 by TGBp2 at 5 dpi; therefore, it is possible that both genes are only partially under the control of *bZIP60*. Thus, silencing *bZIP60* was expected to suppress *BiP* and *SKP1* mRNA.

We employed tobacco rattle virus (TRV)-based virus-induced gene silencing (VIGS) to knock down the expression of *bZIP60*. A 600-bp fragment of *NbbZIP60* was cloned into the TRV vector (Ratcliff et al., 2001; Dong et al., 2007). *N. benthamiana* plants at the four-leaf stage were pretreated with buffer, TRV1 plus TRV2 empty vector, or TRV1 plus TRV2-bZIP60 or TRV1 plus TRV2-SKP1. RNA was harvested from upper leaves of silenced plants 14 d later, and then semiquantitative RT-PCR was carried out to examine the expression of *bZIP60*, *BiP*, and *SKP1* (Fig. 4). As expected, plants that were pretreated with buffer or TRV alone showed similar levels of *bZIP60*, *BiP*, or *SKP1*. In plants treated with TRV2-bZIP60, bZIP60 was suppressed by 77% below mock-treated plants. In plants treated with TRV2-SKP1, SKP1 levels were suppressed 60% below mock-treated plants. We examined *BIP* and *SKP1* expression in *bZIP60*-suppressed plants and found that the expression of these genes was also suppressed 72% and 65%,

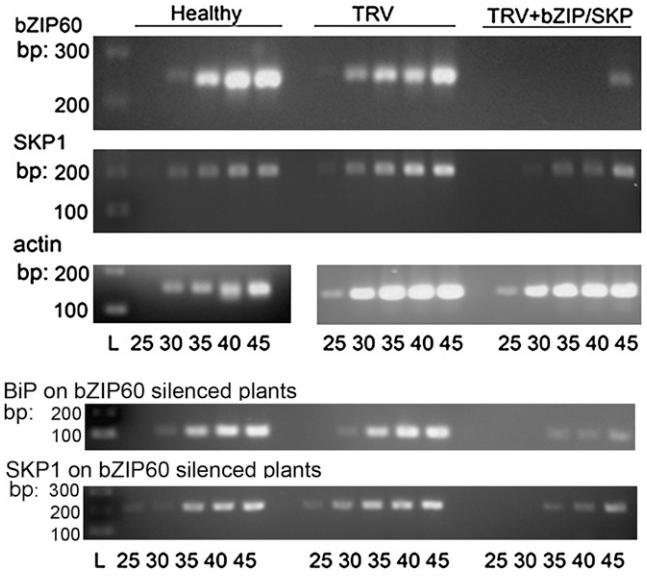

Figure 4. Effects of TRV-bZIP60 on the expression of bZIP60, BiP, and SKP1. Semiquantitative RT-PCR was conducted to verify silencing following TRV-VIGS treatment. The name of the gene analyzed by RT-PCR is listed at the top left of each panel. The sizes in bp of the DNA ladder (L) are indicated on the left. The bottom of each lane indicates the number of PCR cycles performed. PCR bands representing bZIP60, SKP1, and actin (internal control) after 25 cycles are shown for healthy and TRV-treated samples. Below actin are gel panels showing the outcomes of semiquantitative RT-PCR detecting BiP or SKP1 on *bZIP60*-silenced plants. Bands representing BiP are not seen until 45 cycles, and SKP1 bands appear at approximately 35 cycles.

respectively, below mock-treated plants. While we cannot assume that the expression of these genes is solely driven by bZIP60, these data show that knocking down bZIP60 severely hampers BiP and SKP1 expression. Thus, BiP and SKP1 are likely downstream factors regulated by *bZIP60*.

Suppression of bZIP60 and SKP1 Reduces Local Infection and Systemic PVX Movement

We inoculated plants with PVX-GFP and then monitored GFP fluorescence to determine if silencing *bZIP60* interferes with the spread of virus infection throughout the plant. Table I shows that all plants that were pretreated with buffer or TRV produced an average of 26 to 27 infection foci per leaf and became systemically infected with PVX-GFP by 5 dpi. *bZIP60*-silenced plants showed fewer infection foci (average of 18), and only 33% (four of 12) became systemically infected with PVX-GFP at 5 dpi. We noted that 75% of *bZIP60*-silenced plants became infected by 7 dpi, and 100% were infected by 9 dpi (Table I; Fig. 5A). Thus, silencing bZIP60 slowed the spread of virus infection to the upper leaves. This conclusion is further supported by immunoblot analysis performed to detect PVX CP in systemically infected leaves at 7 dpi. PVX accumulation was greatly reduced in *bZIP60*-silenced plants in comparison with buffer- or TRV-pretreated plants (Fig. 5B). These combined data indicate that bZIP60 is a contributing factor to optimum PVX accumulation in systemic tissues.

We also inoculated *SKP1*-silenced plants with PVX-GFP and then monitored GFP fluorescence to determine if SKP1 is vital for the spread of virus infection. There were fewer infection foci (average of 19) on *SKP1*-silenced plants than on buffer- or TRV-pretreated leaves (Table I). This is comparable to the numbers of infection foci occurring on *bZIP60*-silenced plants. At 5 dpi, 50% (six of 12) of *SKP1*-silenced plants were systemically infected with PVX-GFP (Table I). By 7 dpi, all *SKP1*-silenced plants were systemically infected with PVX-GFP. Thus, there is a slight delay in systemic infection compared with control plants (Table I). Immunoblot analysis was performed to detect PVX CP at 7 dpi in systemically infected leaves, and there was no change in comparison with control plants (Fig. 5A).

With respect to *SKP1*-silenced plants, we observed higher GFP fluorescence in upper leaves, although the immunoblot showed that PVX accumulation in systemic tissues was unaltered. Given that SKP1 is a factor contributing to protein turnover, it is possible that silencing *SKP1* reduced the turnover of GFP within infected cells. We have reported increased GFP accumulation in GFP-expressing transgenic leaves treated with a cocktail of proteasome inhibitors, which points to the likelihood that GFP can be a target for the 20S and/or 26S proteasome (Mekuria et al., 2008). We also

Table I. *Local and systemic PVX infection on silenced plants*

Treatment	Average No. of Foci per Leaf[a]	No. Infected at 5 dpi[b]	No. Infected at 7 dpi[b]
Buffer + PVX-GFP	26 ± 9	8/8	8/8
TRV + PVX-GFP	27 ± 11	8/8	8/8
TRV-bZIP60 + PVX-GFP	18 ± 10	4/12	9/12[c]
TRV-SKP1 + PVX-GFP	19 ± 8	6/12	12/12

[a]The average number of green fluorescent infection foci was determined using 16 to 19 leaves at 5 dpi. [b]Total number of systemically infected plants relative to the total number of plants that were inoculated. Plants were scored based on the presence of systemic disease and green fluorescence in the upper leaves. [c]All *bZIP60*-silenced plants were systemic at 9 dpi.

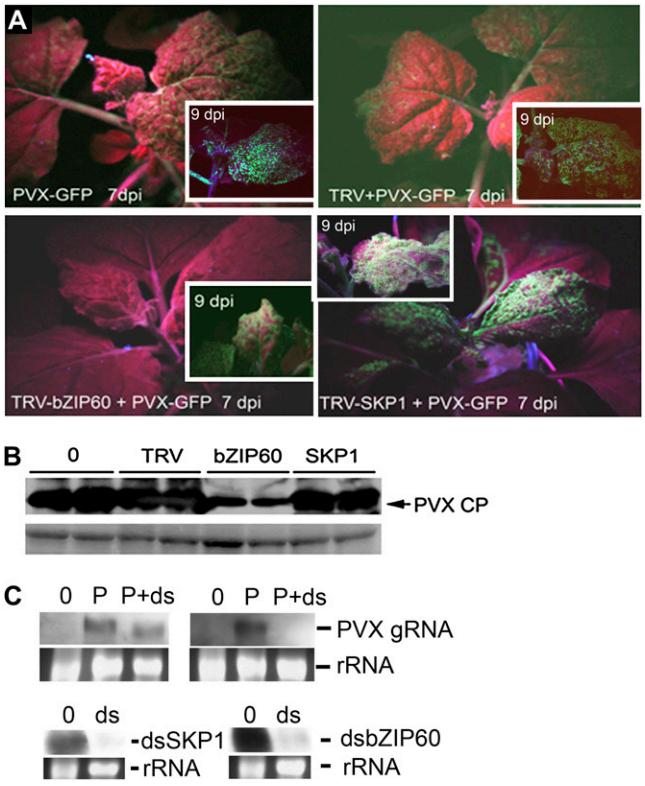

Figure 5. TRV-VIGS-silenced *N. benthamiana* plants were inoculated with PVX-GFP. A, Images of systemic PVX-GFP infection at 7 dpi using a handheld UV lamp. Some plants were pretreated with TRV, TRV-bZIP60, or TRV-SKP1 and then with PVX-GFP at 14 d following TRV delivery. The insets show *bZIP60*-silenced plants with PVX-GFP fluorescence in systemic leaves at 9 dpi. B, Immunoblot analysis confirms PVX CP in infected plants at 7 dpi. Treatment with buffer (0), TRV empty vector, TRV-bZIP60, or TRV-SKP1 is indicated above each pair of lanes. The Coomassie blue-stained gel below the immunoblot shows equal sample loading. C, Northern-blot analysis of BY-2 protoplasts at 36 hpi following transfection with PVX-GFP (P) transcripts and dsRNAs used to knock down *NbSKP1* or *bZIP60* expression. The top of each lane indicates BY-2 protoplasts that are untreated (0), treated with PVX or PVX plus dsRNAs, or treated with dsRNAs alone. Labels on the right indicate RNA probe. An ethidium bromide-stained gel image of rRNA is included below each northern. dsRNAs successfully knocked down SKP1 and bZIP60 expression in BY-2 protoplasts. PVX-GFP accumulation was limited in *bZIP60*-silenced protoplasts but not in *SKP1*-silenced protoplasts.

reported a 5-fold reduction in the steady-state levels of GFP in PVX-GFP-infected protoplasts that were treated with tunicamycin, indicating that GFP turnover may be regulated by UPR machinery (Ju et al., 2008). Tunicamycin is often used as a chemical stimulus of the unfolded protein response (Leborgne-Castel et al., 1999; Surjit et al., 2007). Thus, it is reasonable to consider that the greater intensity of fluorescence may not be an indicator of higher virus titer.

To determine if bZIP60 and SKP1 contribute to virus accumulation in single cells, we delivered synthetic double-stranded (ds) RNAs targeting SKP1 or bZIP60 for silencing (Fig. 5C). Protoplasts were harvested at 36 h post inoculation (hpi), and northern-blot analysis showed high levels of SKP1 and bZIP60 in untreated BY-2 protoplasts but barely detectable levels of the same transcripts in protoplasts treated with dsRNAs. These data indicate that the dsRNAs can successfully knock down host gene expression. PVX-GFP transcripts were delivered to untreated and dsRNA-treated protoplasts, and northern-blot analysis was carried out at 36 hpi. PVX genomic RNA accumulation was unaffected by silencing SKP1 but was significantly impeded in *bZIP60*-silenced protoplasts. These data indicate that bZIP60, but not SKP1, is a factor in virus replication.

Since we show in Figure 4 that bZIP60 might regulate the expression of SKP1 but knocking down each gene has a different outcome in isolated protoplasts, it is arguable that SKP1 does not play the same roll in virus replication as bZIP60. bZIP60 may regulate other genes that directly affect PVX replication in addition to contributing to the regulation of SKP1 expression. In plants, knocking down bZIP60 seems to contribute to reduced or delayed virus systemic accumulation, although knocking down these genes has different effects on GFP intensity in systemic leaves (Fig. 5; Table I). While the data thus far argue that this gene network contributes to PVX infection, based on these limited experiments it is reasonable to propose that bZIP60 regulates more than one gene that contributes to optimum PVX infection. More studies are needed to elaborate the separate roles of bZIP60 and SKP1 in PVX infection.

TGBp3 Expression Does Not Significantly Influence the Turnover of TGB2 or Rep

Many mammalian viruses regulate virus replication via UPR. They encode proteins that insert into the ER membrane and stimulate the UPR, which targets the viral Rep for degradation as a means to down-regulate virus replication late in infection (Yu et al., 2006; Medigeshi et al., 2007). Since PVX Rep, TGBp2, and TGBp3 associate with the ER, we considered the possibility that TGBp3 stimulates the UPR as a means to regulate the turnover of other PVX proteins in the ER. Also, given the differences in GFP intensity when expressed from the PVX genome in *SKP1*-silenced plants, it seemed reasonable to consider that TGBp3 might stimulate cellular UPR to regulate the accumulation of other PVX proteins. To examine this hypothesis, TGBp3His and mycTGBp2 or TGBp3His and mycRep were coexpressed in *N. benthamiana* leaves using agroinfiltration, and immunoblot analysis was used to detect the epitope-tagged proteins at 3 d post infiltration (Fig. 6). Leaves were also infiltrated with *A. tumefaciens* as controls. Consistently high levels of TGBp3-His were detected when it was expressed alone or codelivered with mycTGBp2 or mycRep. TGBp3 did not appear to have a significant impact on the accumulation of mycTGBp2 or mycRep.

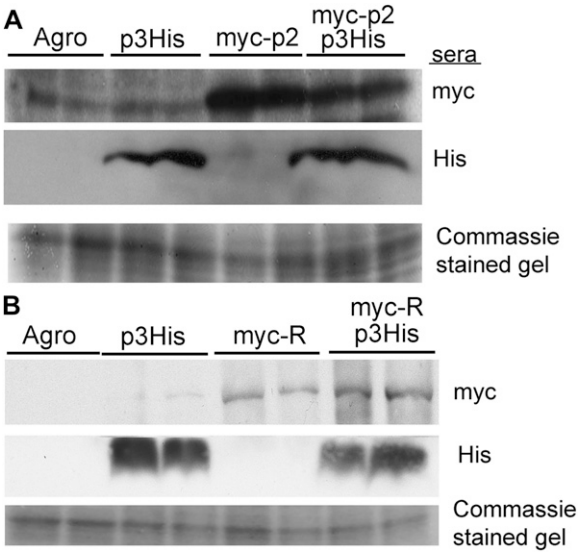

Figure 6. Immunoblot analysis following agroinfiltration with combinations of plasmids expressing TGBp3His, mycTGBp2, and mycRep. A, *N. benthamiana* leaves infiltrated with a suspension of *A. tumefaciens* containing an empty vector (Agro), TGBp3His, mycTGBp2, or mycTGBp2 plus TGBp3His. The top panel shows an immunoblot probed with myc antiserum. The second panel shows an immunoblot probed with His antiserum. The Coomassie blue-stained gel verifies equal loading of samples. B, *N. benthamiana* leaves infiltrated with a suspension of *A. tumefaciens* containing an empty vector, TGBp3His, mycRep, or mycRep plus TGBp3His. The immunoblot in the top panel was probed with myc antiserum and the second panel was probed with His antiserum. The Coomassie blue-stained gel shows equal loading of samples.

Ectopic Expression of TGBp3 Can Lead to Cell Death, Which Can Be Alleviated by BiP Overexpression

We reexamined leaves that were agroinfiltrated with plasmids expressing TGBp3 from the CaMV 35S promoter and noted microscopic necrotic lesions (Fig. 7A) that were absent from control agrodelivery of GUS coding sequences or *A. tumefaciens* alone. Hypersensitive response (HR) necrosis is evident from blue autofluorescence seen under UV light, and reactive oxygen species (ROS) activity was detected using the fluorogenic probe 2′,7′-dichlorofluorescein diacetate (H_2DCFDA; Fig. 7A).

To determine whether BiP is directly responsible for TGBp3-related HR or represents a pathway branch that is induced by TGBp3 alongside the cell death signaling pathway, we overexpressed the *NbBLP-4* (*BiP*) coding sequence from the pBI121 plasmid. *N. benthamiana* leaves were infiltrated with *A. tumefaciens* containing pBI-*NbBLP-4*, pBI121 alone, or buffer and immunoblot analysis was used to compare BiP protein levels among *N. benthamiana* leaves harvested 2 d after infiltration (Fig. 7B). The density of bands reporting BiP expression was 3-fold higher in *NbBLP-4* infiltrated leaves than in buffer-treated leaves (data not shown). This level of overexpression is within the range reported at 3 dpi for PVX-infected leaves and agroinfiltrated leaves expressing TGBp3.

We agroinfiltrated leaves delivering BiP alone (pBI-*NbBLP-4*), TGBp3 alone, or a mixture of *A. tumefaciens* expressing BiP and TGBp3 (Fig. 7C). BiP overexpression was sufficient to alleviate TGBp3-induced necrosis (Fig. 7C). Using a UV lamp and H_2DCFDA staining, necrosis was seen only in TGBp3-expressing leaves.

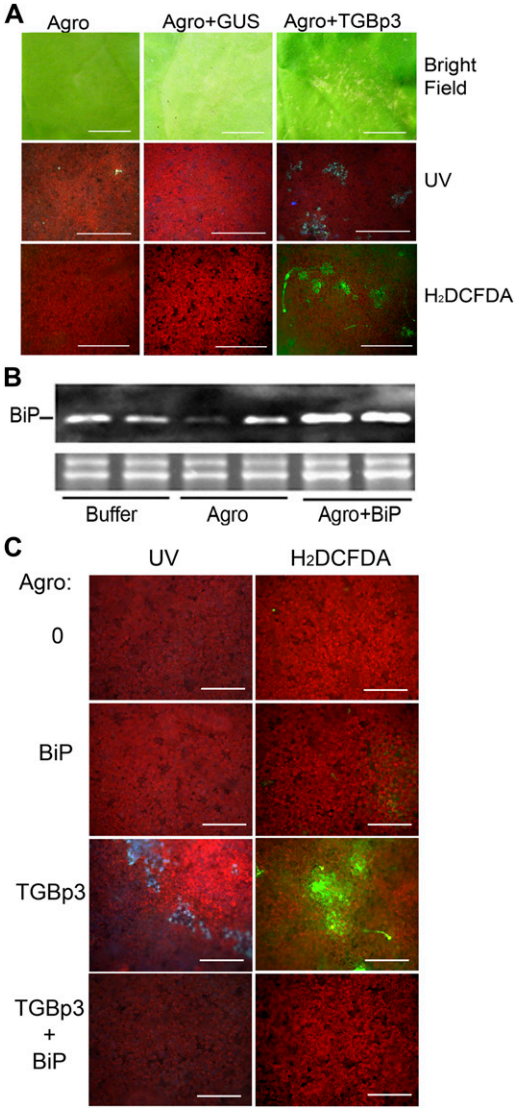

Figure 7. Overexpression of BiP alleviates TGBp3-induced cell death. A, *N. benthamiana* leaves infiltrated with *A. tumefaciens* alone, containing a GUS construct, or TGBp3 fused to CaMV 35S promoter. The bright-field images show necrotic flecks. Bars = 50 μm. B, Immunoblot detection of *BiP* in leaf extracts at 2 d post infiltration. The image shows bright bands corresponding to immunodetected proteins. Films were scanned, and reverse images were recorded for high-resolution visualization of bands. The Coomassie blue-stained membrane shows equal amounts of protein loaded in each lane. C, *N. benthamiana* leaves infiltrated with *A. tumefaciens* listed on the left of each pair of panels. The left column shows necrosis seen under a UV lamp, and the right column shows similar tissues following treatment with H_2DCFDA stain, which detects ROS activity. Bars = 50 μm.

Codelivery of BiP eliminated necrosis and evidence of ROS (Fig. 7C). These data concur with earlier findings that BiP is up-regulated upon pathogen invasion as a response to the increase in protein translation but is not directly responsible for the HR (Jelitto-Van Dooren et al., 1999). Importantly, the fact that necrosis is abrogated by *BiP* overexpression clearly demonstrates that TGBp3-related cell death is linked to ER stress. Given that Figure 4 shows that bZIP60 is a factor regulating BiP expression as well as SKP1, these data argue that bZIP60 and BiP might play a role in regulating cytotoxic effects of PVX proteins during virus infection. Limiting protein cytotoxicity might be important for enabling optimal systemic virus spread by reducing tissue necrosis.

DISCUSSION

Here, we report that *bZIP60*, several plant UPR-related ER-resident chaperones, and the Cullin cochaperone *SKP1* are induced following PVX infection or *A. tumefaciens* delivery of TGBp3 to *N. benthamiana* or Arabidopsis plants. Evidence that PVX infection and ectopically expressed TGBp3 up-regulate *bZIP60*, *SKP1*, and ER resident chaperones such as *BiP* is intriguing and provides, to our knowledge, the first clear evidence that a plant viral protein elicits the UPR and a factor (SKP1) linked to proteasome-dependent pathways. Such comparisons of Arabidopsis and *N. benthamiana* gene expression in response to TGBp3 delivery are significant because they demonstrate that this is not a host-specific response and that there are general implications for host-virus interactions. Unfortunately, the incomplete representation of host genes on the microarrays and the lack of the complete *N. benthamiana* genome sequence hinder the identification of orthologous genes or the explanation of why certain genes, such as bZIP factors, were not identified in Arabidopsis although they were identified in the potato microarrays. However, in a broader context, the data show that members of gene families encoding ER-resident proteins can be induced to similar levels (between 2- and 5.5-fold) in both species.

bZIP60 belongs to a class of membrane-bound ER stress sensors that are responsible for up-regulating genes involved in the UPR (Supplemental Fig. S1; Iwata and Koizumi, 2005a; Urade, 2007; Lu and Christopher, 2008). bZIP60 is activated by ER stress and regulated by intramembrane proteolysis. Cleavage of the full-length protein by a noncanonical proteolytic event releases the transcription factor from the ER (Iwata et al., 2008, 2009). The truncated bZIP60 activates promoters containing cis-elements, P-UPRE and ERSE, which are responsible for ER stress response, including activating its own transcription and *BiP* genes (Seo et al., 2008; Urade, 2009; Fig. 1). bZIP60-regulated UPR is potentially a factor in promoting optimal PVX accumulation in infected protoplasts and plants by (1) reducing cytotoxicity that can lead to necrosis and (2) regulating the expression of cellular factors contributing to virus infection. These conclusions are based on critical observations. First, our observations that agroinfiltration of *NbBLP-4* eliminated TGBp3-induced HR confirmed a cytoprotective role for BiP in virus-infected leaves and for controlling TGBp3-induced ER stress (Fig. 1; Iwata et al., 2008; Lu and Christopher, 2008; Urade, 2009). These experiments suggest that PVX employs the UPR machinery, via TGBp3 and BiP, to regulate cytotoxic damage to the cell as a means to promote virus spread. UPR is reported to be a component of important early responses to pathogen invasion in anticipation of the increase in protein synthesis along the ER but is not directly responsible for defense gene induction (Jelitto-Van Dooren et al., 1999). In particular, BiP is a well-known component of cellular cytoprotective responses to alterations in the ER or the accumulation of misfolded proteins and controls the status of certain UPR transmembrane signal transducers (e.g. IRE1, PERK, and ATF6; Tardif et al., 2004; Zhang and Kaufman, 2006). Leborgne-Castel et al. (1999) were the first to demonstrate that mild overexpression of BiP (*NbBLP-4*) in transgenic plants restores ER homeostasis and protects plants from ER stress (Costa et al., 2008). Importantly, *AtHSP70* induction is also linked to plant protein overexpression. BiP is a member of the HSP70 multigene family, and a subset of cytoplasmic *AtHSP70* genes (*HSC70-1*, *-2*, *-3*, and *HSP70* but not *AtHSP70B*) are induced as part of a general response to viral protein accumulation (Whitham et al., 2003; Aparicio et al., 2005). Thus, HSP70 may contribute to modulating cellular stresses during virus infection in a manner that is reminiscent of the UPR (Aparicio et al., 2005). Our study contrasts with the prior work on HSP70 by presenting several experimental outcomes that point to TGBp3 as a specific inducer of BiP expression.

To support the notion that UPR is a factor regulating disease, we inoculated *bZIP60*- and *SKP1*-silenced plants and protoplasts with PVX-GFP. We report fewer infection foci on *bZIP60*- and *SKP1*-silenced *N. benthamiana* plants, suggesting that PVX infection was attenuated by the greatly reduced *bZIP60* or *SKP1* expression. The reduced number of green fluorescent infection foci (Table I) and reduced PVX genomic RNA accumulation in protoplasts correlated with the dramatic reduction in *bZIP60* transcript accumulation. These data suggest that *bZIP60* is a factor contributing to PVX-GFP replication in protoplasts and *N. benthamiana* leaves. The partial inhibition of bZIP60 expression in *N. benthamiana* plants did not compare with the inhibition seen in protoplasts. Therefore, new research tools are needed to improve the knockdown of bZIP60 in *N. benthamiana* plants or other hosts of PVX to examine the contribution of *bZIP60* to promoting long-distance PVX spread. It is worth considering bZIP60 as a target for developing a transgenic approach to virus resistance.

SKP1 is an essential component of the SCF family of E3 ubiquitin ligases, which provides substrate ubiq-

uitination preceding proteasome-mediated degradation (Cardozo and Pagano, 2004; Petroski and Deshaies, 2005). Typical substrates are cellular proteins crucial for eukaryotic physiology and defense. In Figure 2, we report that PVX infection and TGBp3 up-regulate *SKP1* mRNA expression, but it is not clear if increased *SKP1* expression is necessary to degrade viral proteins or simply to alleviate the congestion of proteins in the ER by enhancing protein turnover. We also noticed that *SKP1* is up-regulated by TGBp2 at 5 dpi, although TGBp2 does not appear to be impacted by *bZIP60* expression. We also show that silencing *bZIP60* can alter the expression of *SKP1* in the absence of a viral inducer, which suggests that these genes are linked in a pathway. But failure to completely shut down *SKP1* expression, combined with evidence that TGBp2 can induce *SKP1*, raises the possibility that *SKP1* may be controlled by additional factors and may not be completely controlled by bZIP60. Further analyses are needed to detail the relationship of these genes. This would require cloning the *SKP1* promoter and analyzing the elements that control gene expression. For example, it would be interesting to learn if the *SKP1* promoter has P-UPRE and ERSE elements and may be recognized by other bZIP transcription factors.

Evidence linking TGBp3 to SKP1 is exciting, given recent reports linking proteasomal activities to systemic virus movement and to the functions of certain plant viral silencing suppressor proteins. For example, RPN9 is a proteasomal subunit whose expression is required for systemic movement of *Tobacco mosaic virus* and *Turnip mosaic virus*. Silencing RPN9 seemed to generally impede virus systemic movement, although the protein also seems to play a role in appropriate vascular development (Jin et al., 2006). More closely related to this work is evidence that the beet western yellow virus P0 silencing suppressor has an F-box domain and directly binds SKP1 orthologs in Arabidopsis, although the cellular components of the silencing machinery that are targeted by the SCF E3 ubiquitin ligase are not known (Baumberger et al., 2007). However, silencing *SKP1* in *N. benthamiana* caused plants to become resistant to beet western yellow virus infection, indicating that the relationship of P0 and SKP1 is vital for virus spread. We report here that silencing *SKP1* reduced the number of infection sites on inoculated leaves and the number of infected plants (Table I), suggesting that it plays a role in PVX infection. Moreover, the PVX TGBp1 silencing suppressor targets AGO1, which is the effector nuclease of the RNA silencing machinery, for degradation via the proteasome (Chiu et al., 2010). Thus, combining this work with previous reports on TGBp1, it is possible that TGBp3 up-regulates UPR and components of the ubiquitin-proteasome pathway to enable the degradation of AGO1 mediated by TGBp1. Thus, the TGBp1 and TGBp3 proteins might act in concert to regulate host defense and stress responses in a manner that renders plants more susceptible to PVX infection. Further research is needed to determine the link between TGBp1, TGBp3, and proteasomal degradation of cellular components of the silencing machinery.

Moreover, this outcome suggests a role for the UPR in promoting virus spread and raises the question of how bZIP60, UPR, as well as cellular events required to maintain ER homeostasis regulate systemic PVX accumulation. There are three possible explanations. First, bZIP60 could play a direct role in PVX infection that is unrelated to its role in UPR induction. This explanation seems unlikely, given that bZIP60 is responsible for the up-regulation of ER-resident chaperones such as BiP (Iwata and Koizumi, 2005a; Lu and Christopher, 2008), and we show that BiP plays a role in suppressing TGBp3-related ER stress. Second, bZIP60 might up-regulate another gene whose protein product is a positive factor in promoting virus replication and movement. Further experiments are needed to identify additional bZIP60-regulated factors and assess their role in PVX movement. Third, bZIP60 might be required to enhance cellular protein-folding abilities (perhaps by increasing BiP expression), proteasomal function for degradation of AGO1, and ER membrane synthesis necessary for optimal virus accumulation. This latter possibility is based on the flavivirus model. The nonstructural proteins of JEV and DEN-2 trigger the ER-resident sensors that lead to signaling pathways that enhance cellular protein-folding abilities, ER membrane synthesis, and up-regulation of the secretory system (Urano et al., 2000). These events are necessary to manage the increase in protein translation resulting from virus infection and provide further membranes needed for replication and maturation (Yu et al., 2006). During PVX infection, expansion of the ER network is known to be important for virus infection. Cells treated with cerulenin, an inhibitor of membrane synthesis, supported reduced virus replication (Bamunusinghe et al., 2009). Thus, the preliminary data point to the possibility that PVX, similar to flaviviruses, triggers the UPR to enhanced cellular protein-folding abilities and ER membrane synthesis. If SKP1 expression is regulated by bZIP60, then there is additional regulation of the proteasomal pathway that might be important for effective silencing suppression mediated by TGBp1. These combined events could be necessary to promote virus cell-to-cell movement.

Similarly, buildup of viral proteins in the ER or the retention of inefficiently folded viral envelope proteins in the ER is cytotoxic and leads to UPR initiation by mammalian viruses such as HCV, JEV, human cytomegalovirus, and bornavirus (Chan and Egan, 2005; Williams and Lipkin, 2006). In these examples, viral proteins trigger ER stress in a manner that leads to cell death only when the protein load in the ER exceeds the folding capacity induced by ER stress. When we compare the effects of expressing TGBp3 at various levels, it becomes worth considering that the amounts of TGBp3 expressed during PVX infection are tightly regulated to avoid damaging the cells. Given that TGBp3 is expressed from the PVX genome via a subgenomic

RNA at low levels, this may be necessary to promote virus spread by preventing cytotoxic cell death.

There are intriguing similarities between PVX TGBp3 and the human immunodeficiency virus (HIV) Vpu protein. Both proteins are expressed from bicistronic mRNAs, and they have low molecular masses with single transmembrane domains that insert into the ER. Vpu binds to the cellular CD4 protein in the ER and recruits the human F-box protein βTrCP targeting CD4 for degradation via the ubiquitin-proteasome pathway. CD4 is a cell surface receptor required for HIV uptake into cells, and the process of dislocation and degradation of CD4 in the ER reduces the number of available receptors at the cell surface and is important to free HIV gp160 in the ER for virus maturation and trafficking (Bour et al., 1995; Schubert et al., 1998; Malim and Emerman, 2008; Nomaguchi et al., 2008). It is worth considering that TGBp3 might function to bind cellular proteins and recruit them to the ubiquitin-proteasome pathway. PVX TGBp3 might function in the ER to down-regulate host factors contributing to virus replication or early stages of infection during their translation, which could be essential for maintaining virus infection and promoting cell-to-cell spread. Further experiments are needed to identify host proteins interacting with TGBp3 and its ability to associate with components of the SCF complex.

CONCLUSION

For the last 15 years, plant virologists have reported viral movement proteins embedded in the ER. Until now, researchers have viewed the ER as a location for the assembly and lateral transport of movement complexes toward plasmodesmata, but there have been no reports indicating a role for the ER or the UPR in promoting plant virus spread. This is in contrast to significant advances on this topic that have been made in mammalian virus research. The data presented in this study point to a new role for the ER in regulating plant virus movement. We provide to our knowledge the first evidence linking UPR to systemic accumulation of PVX and raise the possibility that *bZIP60* is an important factor in PVX infection. This study of the ER-resident PVX TGBp3 protein will open the door to further examination of whether PVX employs machinery similar to the ER-resident proteins encoded by flaviviruses or retroviruses, such as HIV, to modulate various ER stress responses as a means to cope with robust viral protein synthesis (Tardif et al., 2004; Chan and Egan, 2005; Medigeshi et al., 2007; Alwine, 2008; Surjit and Lal, 2008), increase membrane biosynthesis needed for virus replication and maturation, prevent superinfection, and modulate cell death functions.

MATERIALS AND METHODS

Plasmids and Bacterial Strains

pGR208, a binary vector containing the PVX-GFP genome, was obtained from Dr. P. Moffett. pGR208 is deliverable to plants by agroinfiltration.

A 6x-His tag (underlined) was introduced at the 3′ end of the PVX TGBp3 coding sequence in pTXS-GFP plasmids using the Quick-Change II XL Site-Directed Mutagenesis Kit (Stratagene) with forward primer 5′-GTTGACGGTTAAGTTTCACCATCACCATCACCATTGATACTCGAAAG-3′ and reverse primer 5′-CTTTCGAGTATCAATGGTGATGGTGATGGTGAAACTTAACCGTTCAAC-3′. The reaction products were transformed into *Escherichia coli* XL10-Gold.

Agrobacterium tumefaciens deliverable binary vectors were prepared using pMDC32 plasmids and Gateway technology with Clonase II (Invitrogen). The pMDC32 contains the CaMV 35S promoter. To generate pMD32-TGB3His, the TGB3His DNA fragment was first amplified using an attB1 primer (5′-GGGGACAAGTTTGTACAAAAAAGCAGGCTTCGGATCCATGGAAGTAAATACATATC-3′) and an attB2 primer containing the 6x-His tag (underlined; 5′-GGGGACCACTTTGTACAAGAAAGCTGGGTCTCAGTGGTGATGGTGATGATGGAAACTTAACCGTTCAAC-3′). To generate pMD32-TGBp1 and CP, PCR fragments were amplified using attB1 primers 5′-GGGGACAAGTTTGTACAAAAAAGCAGGCTGTATGGATATTCTCATCAGTAG-3′ and 5′-GGGGACAAGTTTGTACAAAAAAGCAGGCTGTATGTCAGCACCAGCTAGC-3′ and aatB2 primers 5′-GGGGACCACTTTGTACAAGAAAGCTGGGTGCTATGGCCCTGCGCGGACAT-3′ and 5′-GGGGACCACTTTGTACAAGAAAGCTGGGTGTTATGGTGGTGGTAGAGTGAC-3′. The DNA fragments were incubated with pDONR/zeo and BP Clonase II for 1 h. Then pMDC32 binary vector (obtained from Dr. R. Sunkar, Oklahoma State University) and LR Clonase II were added to the reaction mix and incubated for 1 h. The reaction products were transformed to One Shot OmniMax2-T1-competent *E. coli* cells. After sequencing confirmation of the derived plasmids, the pMDC32-TGBp3his plasmid was used to transform *A. tumefaciens* strain GV2260. A set of plasmids was also prepared replacing the CaMV 35S promoter with the NOS promoter. A total of 307 nucleotides of the NOS promoter were was amplified from the pBI121 plasmid using the forward primer 5′-GCAAGCTTGATCATGAGCGGAGAATTAAG-3′ (the *Hin*dIII site is underlined) and the reverse primer 5′-GCGGTACCAGATCCGGTGCAGATTATTTGG-3′ (the *Kpn*I site is underlined). The PCR fragment was cloned into pMDC-p3H between *Hin*dIII and *Kpn*I to replace its CaMV 35S promoter.

The *A. tumefaciens* deliverable pGWB21 binary vector (obtained from Dr. T. Nakagawa, Shimane University) includes an 11x-myc tag at the 5′ end of the inserted open reading frames. PVX TGBp2 and Rep coding sequences were cloned into pGWB21 using the same Gateway technology described above. To generate pGWB21-mycTGB2, TGB2 was PCR amplified using a forward attB1 primer containing the myc tag (underlined; 5′-GGGGACAAGTTTGTACAAAAAAGCAGGCTTCGGATCCATGGAACAAAAAATTTCTAAGATCTGTCCGCGCAGGGCCATAGG-3′) and a reverse attB2 primer (5′-GGGGACCACTTTGTACAAGAAAGCTGGGTACTACTAATGACTGCTATGATTGTTACC-3′). To generate pGWB21-mycRep, the PVX Rep was PCR amplified using a forward attB1 primer containing the myc tag (underlined; 5′-GGGGACAAGTTTGTACAAAAAAGCAGGCTTGATGAACAGAAACTTATTTCTGGAAGAAGATCTGGCCAAGGTGCGCGAGGTT-3′) and a reverse attB2 primer (5′-GGGGACCACTTTGTACAAGAAAGCTGGGTCTTAAAGAAAGTTTCTGAGGCG-3′). After sequencing confirmation, pGWB21-mycTGBp2 and pGWB21-mycRep were transformed to *A. tumefaciens* strain GV2260.

A. tumefaciens LBA4404 containing pBI-*BLP4* was prepared by inserting the coding sequence between the *Xba*I and *Sac*I restriction sites of pBI121 plasmids (Jefferson et al., 1987). Total RNA was extracted from *Nicotiana benthamiana* leaves using Trizol Reagent (Invitrogen) and treated with DNase I (Promega). *NbBLP-4* coding sequence (accession no. FJ463755.1) was synthesized with SuperScript Reverse Transcriptase III (Invitrogen) and amplified by Pfu Turbo DNA polymerase (Stratagene). *NbBLP-4* cloning primers were designed based on *NtBLP-4* (accession no. X60057; Supplemental Table S1). *NbBLP-4* showed greater than 98% homology with the *NtBLP-4* cDNA (Leborgne-Castel et al., 1999). *NbBLP4* cDNA was cloned into pGEM-T Easy vector (Promega) and sequenced with M13 primers. The plasmid pRTL2.TGBp3-GFP was prepared previously (Samuels et al., 2007). TGBp3Dm1-GFP was PCR amplified using primers containing *Nco*I and *Bam*HI restriction sites and then inserted into pRTL2 plasmids.

A. tumefaciens strain GV2260 containing TRV1 plus TRV2-NbSKP1, TRV2-bZIP60, TRV2-PDS, or TRV2-GFP was provided by Dr. S. Dinesh-Kumar (Yale University; Liu et al., 2004; Bhattarai et al., 2007). The *NtbZIP60* gene fragment (nucleotides 168–776 of the *NtbZIP60* coding sequence) was cloned into pDONR/zeo and pTRV2 Gateway vectors with Gateway Clonase II (Invitrogen) with forward primer attB1 (5′-GGGGACAAGTTTGTACAAAAAAGCAGGCTGTCGGTCACGTGGCTGTC-3′) and reverse primer attB2 (5′-GGGGACCACTTTGTACAAGAAAGCTGGGTGGAACCAGAAGACCGTGG-3′).

Plant Materials and Inoculations

N. benthamiana and Arabidopsis (*Arabidopsis thaliana*) plants were used. Purified virus was prepared from infected *N. benthamiana* plants using the traditional methods and suspended in 0.01 M phosphate buffer (pH 7.0; Shadwick and Doran, 2007). Virus concentration (C) was determined by measuring OD_{260} and calculated by the formula $C = OD_{260}/3.0$. Aliquots of viruses were stored at −80°C, and then 30 μg mL^{-1} virus was used for each inoculation.

Agroinfiltration for plasmid or TRV delivery to *N. benthamiana* or Arabidopsis leaves was performed with a 1-mL needle-free syringe according to published protocols (Liu et al., 2002). *A. tumefaciens* LBA4404 or GV2260 infiltrations were conducted using 10 plants for each treatment, and infiltration medium (buffer) was used as a negative control. *A. tumefaciens* cultures were collected by centrifugation and resuspended in agroinfiltration solution (10 mM $MgCl_2$, 10 mM MES, pH 7.0, and 200 μM acetosyringone). The suspension was adjusted to OD_{600} = 1.0, 0.1, or 0.01 and infiltrated to *N. benthamiana* leaves with a 1-mL needle-free syringe. *N. benthamiana* plants were grown to the four-leaf stage for infiltration. GV2260 cells were also infiltrated to leaves, serving as the negative control.

H_2DCFDA Staining of Leaf Segments

N. benthamiana plants were agroinfiltrated and ROS activity was detected using the fluorogenic probe H_2DCFDA (Mahalingam et al., 2006). For visual assessment of ROS activity, leaf samples were treated with 50 μM H_2DCFDA for 20 min and observed using a Nikon E600 epifluorescence microscope.

Immunoblot Analyses

For immunoblot analysis of virus-infected or agroinfiltrated leaves, 0.3 g of treated leaf samples was harvested from inoculated leaves at 5 dpi or from upper leaves at 8 to 10 dpi. Total protein was extracted from leaves by grinding samples with extraction buffer (4 M urea, 4% SDS, 0.2 M dithiothreitol, 20% glycerol, 0.2 M Tris-HCl, pH 6.8, and 0.04% bromphenol blue; Draghici and Varrelmann, 2009) or standard protein extraction buffer (100 mM Tris-HCl, pH 7.5, 10 mM KCl, 0.4 M Suc, 10% glycerol, and 10 μM phenylmethylsulfonyl fluoride; Sambrook et al., 1989) and quantified using Bradford Reagent (Sigma-Aldrich). Thirty micrograms of protein for each sample was loaded onto a 4% to 20% precast gradient or 10% SDS-PAGE gels (Bio-Rad) and electroblotted to Hybond-P (GE Healthcare) using standard protocols (Sambrook et al., 1989). Blots were probed with BiP (GRP78) antiserum (Affinity BioReagents), 5x-His monoclonal IgG (Qiagen), c-Myc monoclonal IgG (Santa Cruz Biotechnology), PVX CP (Agdia), or GFP polyclonal antiserum (Affinity BioReagents). Horseradish peroxidase-conjugated goat anti-mouse IgG (Jackson ImmunoResearch Laboratories) served as the secondary antiserum using the ECL Advanced Western Blotting Kit (GE Healthcare). Blots were exposed to film for 10 to 60 s. Film was scanned using the alpha Image imaging system (α Innotech), and the reverse image was recorded. Densitometric analysis was performed by alpha Ease FC software (α Innotech). Films were scanned and images were cropped with the CanonScan 9950F scanner and associated program Arcsoft Photo Studio 5 (Canon).

qRT-PCR Analysis of Infected Leaves and Semiquantitative RT-PCR of Silenced Plants

Mock-inoculated (treated with agroinfiltration buffer) plants were used as a control and calibrator sample. The SV Total RNA Isolation kit (Promega) was used to extract total RNA from samples. The first-strand cDNA was synthesized by SuperScript Reverse Transcriptase III (Invitrogen) using hexamer random primers. qPCR was carried out using 25-μL reactions and 100 to 900 nM primers designed using the coding sequences for known Arabidopsis, tobacco (*Nicotiana tabacum*), or *N. benthamiana* genes (Supplemental Table S1). Initial RT-PCR tests of the gene-specific primers confirmed their ability to amplify single bands of the predicted sizes from *N. benthamiana* cDNA. A total of 25 ng of cDNA was used to perform qPCR using the Power SYBR Green II Master Mix and ABI 7500 PCR machine (Applied Biosystems). Reactions were incubated first at 95°C for 10 min and then for 40 cycles of 95°C for 15 s and 60°C for 60 s. Efficiencies of all primers were verified by normal RT-PCR and gel electrophoresis. The comparative C_T method was employed for relative quantitation of gene expression following virus treatments. qRT-PCR efficiencies were determined by control amplifications using 0.01, 0.1, 1, 10, and 100 ng of template cDNA. Duplicate PCRs for each sample were carried out and averaged. The comparative C_T method employs the equation 2^{-ddCT}, where the values of the endogenous control (18S RNA) and calibrator (a constant quantity of a healthy sample template) are subtracted from the target sample value to provide the ddC_T value. The equation 2^{-ddCT} represents the fold of RNA accumulation.

Semiquantitative RT-PCR *NbSKP1* and *bZIP60* primers were designed to anneal outside the target sequence of VIGS (Liu et al., 2002). To detect the *SKP1*- or *bZIP60*-silencing effect, total RNA was extracted from agroinfiltrated *N. benthamiana* leaves at 14 d post infiltration with the SV Total RNA Isolation System (Promega). The first-strand cDNA was synthesized with SuperScript III Reverse Transcriptase (Invitrogen), 1 μg of total RNA, and 100 μM 6-mer random primers. *bZIP60* semiquantitative RT-PCR was performed with bZIP60 primers 5′-CCTGCTTTGGTTCATGGGCATCAT-3′ (forward; nucleotides 672–695) and 5′-CACATCACAATTCCCAAATAATG-3′ (reverse; nucleotides 877–900). For amplification of *NbSKP1*, we employed forward primer 5′-TGACATGCCAGACAGTTGCAGACA-3′ (nucleotides 303–326) and reverse primer 5′-TTCGATCTCATCCTGGCT-3′ (nucleotides 439–462). *N. benthamiana* actin primers 5′-AAAGACCAGCTCATCCGTGGAGAA-3′ (forward) and 5′-TGTGGTTTCATGAATGCCAGCAGC-3′ (reverse) were used to amplify actin as the internal control. Semiquantitative RT-PCR was performed with the same protocols described above.

Preparation of BY-2 Protoplasts, dsRNA Delivery, and Northern-Blot Analysis

BY-2 protoplasts were prepared and transfected as described previously (Lee et al., 2008). Two micrograms of *NbSKP1* or *NtbZIP60* dsRNA and 25 μg of PVX-GFP transcripts were delivered to 1×10^6 protoplasts. Transfected BY-2 cells were incubated at 25°C, and then total RNA was extracted at 48 h using Trizol Reagent (Invitrogen). Total RNA (15 μg) was subjected to northern-blot detection with the North-2-South Chemiluminescent Hybridization and Detection Kit (Pierce Biotechnology).

PVX-GFP transcripts were prepared using standardized protocols that were reported previously (Bamunusinghe et al., 2009). dsRNAs were prepared as described previously (Qi et al., 2004; Silva et al., 2010). A PCR fragment of *NbSKP1* coding sequence (nucleotides 21–457) and a fragment of *NtbZIP60* coding sequence (nucleotides 168–776) were cloned into pGEM-T Easy (Promega). The plasmids were linearized using *Spe*I, and positive sense transcripts were synthesized using the RiboMAX Large Scale RNA Production System-T7 (Promega). Plasmids were also linearized using *Nco*I, and then negative sense transcripts were synthesized using the RiboMAX Large Scale RNA Production System-SP6 (Promega). DNA was removed by digestion for 15 min using DNase I. Transcripts were precipitated and then resuspended in RNase-free distilled, deionized water. Equal amounts of positive- and negative-strand RNAs were mixed in annealing buffer (100 mM potassium acetate, 4 mM $MgCl_2$, and 60 mM HEPES-KOH, pH 7.4) and incubated overnight at 37°C to produce dsSKP1 or dsbZIP60 RNA.

Probes for northern blots were prepared by adding 100 ng of NbSKP1, NtbZIP60, or PVX CP PCR fragments to a random priming reaction (North-2-South Biotin Random Prime Labeling Kit; Pierce Biotechnology). Blots were incubated overnight with each probe at 55°C and developed using Kodak Biolight film.

Sequence data from this article can be found in the GenBank/EMBL data libraries under accession number FJ463755.1.

Supplemental Data

The following materials are available in the online version of this article.

Supplemental Figure S1. Mammalian and plant UPR pathways.

Supplemental Table S1. Genes identified by microarray analysis.

ACKNOWLEDGMENTS

We thank Dr. Peter Moffett (University of Sherbrooke), Dr. Ramamurthy Mahalingam (Oklahoma State University), and Drs. K. Mysore and S.R.

Uppalapati (Noble Foundation) for biomaterials. We also thank Dr. J. Carr (Cambridge University) for insightful discussions.

Received February 10, 2011; accepted April 4, 2011; published April 6, 2011.

LITERATURE CITED

Alwine JC (2008) Modulation of host cell stress responses by human cytomegalovirus. Curr Top Microbiol Immunol **325:** 263–279

Aparicio F, Thomas CL, Lederer C, Niu Y, Wang D, Maule AJ (2005) Virus induction of heat shock protein 70 reflects a general response to protein accumulation in the plant cytosol. Plant Physiol **138:** 529–536

Bamunusinghe D, Hemenway CL, Nelson RS, Sanderfoot AA, Ye CM, Silva MA, Payton M, Verchot-Lubicz J (2009) Analysis of potato virus X replicase and TGBp3 subcellular locations. Virology **393:** 272–285

Baumberger N, Tsai CH, Lie M, Havecker E, Baulcombe DC (2007) The Polerovirus silencing suppressor P0 targets ARGONAUTE proteins for degradation. Curr Biol **17:** 1609–1614

Bhattarai KK, Li Q, Liu Y, Dinesh-Kumar SP, Kaloshian I (2007) The *MI-1*-mediated pest resistance requires Hsp90 and Sgt1. Plant Physiol **144:** 312–323

Bour S, Schubert U, Strebel K (1995) The human immunodeficiency virus type 1 Vpu protein specifically binds to the cytoplasmic domain of CD4: implications for the mechanism of degradation. J Virol **69:** 1510–1520

Cardozo T, Pagano M (2004) The SCF ubiquitin ligase: insights into a molecular machine. Nat Rev Mol Cell Biol **5:** 739–751

Chan SW, Egan PA (2005) *Hepatitis C virus* envelope proteins regulate *CHOP* via induction of the unfolded protein response. FASEB J **19:** 1510–1512

Chiu MH, Chen IH, Baulcombe DC, Tsai CH (2010) The silencing suppressor P25 of Potato virus X interacts with Argonaute1 and mediates its degradation through the proteasome pathway. Mol Plant Pathol **11:** 641–649

Costa MD, Reis PA, Valente MA, Irsigler AS, Carvalho CM, Loureiro ME, Aragão FJ, Boston RS, Fietto LG, Fontes EP (2008) A new branch of endoplasmic reticulum stress signaling and the osmotic signal converge on plant-specific asparagine-rich proteins to promote cell death. J Biol Chem **283:** 20209–20219

Denecke J, Carlsson LE, Vidal S, Höglund AS, Ek B, van Zeijl MJ, Sinjorgo KM, Palva ET (1995) The tobacco homolog of mammalian calreticulin is present in protein complexes in vivo. Plant Cell **7:** 391–406

Denecke J, Goldman MH, Demolder J, Seurinck J, Botterman J (1991) The tobacco luminal binding protein is encoded by a multigene family. Plant Cell **3:** 1025–1035

Dong Y, Burch-Smith TM, Liu Y, Mamillapalli P, Dinesh-Kumar SP (2007) A ligation-independent cloning tobacco rattle virus vector for high-throughput virus-induced gene silencing identifies roles for NbMADS4-1 and -2 in floral development. Plant Physiol **145:** 1161–1170

Draghici HK, Varrelmann M (2009) Evidence that the linker between the methyltransferase and helicase domains of potato virus X replicase is involved in homologous RNA recombination. J Virol **83:** 7761–7769

Ellgaard L, Helenius A (2003) Quality control in the endoplasmic reticulum. Nat Rev Mol Cell Biol **4:** 181–191

García-Marcos A, Pacheco R, Martiáñez J, González-Jara P, Díaz-Ruíz JR, Tenllado F (2009) Transcriptional changes and oxidative stress associated with the synergistic interaction between Potato virus X and Potato virus Y and their relationship with symptom expression. Mol Plant Microbe Interact **22:** 1431–1444

Gfeller A, Liechti R, Farmer EE (2010) Arabidopsis jasmonate signaling pathway. Sci Signal **3:** cm4

Iwata Y, Fedoroff NV, Koizumi N (2008) *Arabidopsis* bZIP60 is a proteolysis-activated transcription factor involved in the endoplasmic reticulum stress response. Plant Cell **20:** 3107–3121

Iwata Y, Koizumi N (2005a) An Arabidopsis transcription factor, AtbZIP60, regulates the endoplasmic reticulum stress response in a manner unique to plants. Proc Natl Acad Sci USA **102:** 5280–5285

Iwata Y, Koizumi N (2005b) Unfolded protein response followed by induction of cell death in cultured tobacco cells treated with tunicamycin. Planta **220:** 804–807

Iwata Y, Yoneda M, Yanagawa Y, Koizumi N (2009) Characteristics of the nuclear form of the Arabidopsis transcription factor AtbZIP60 during the endoplasmic reticulum stress response. Biosci Biotechnol Biochem **73:** 865–869

Jefferson RA, Kavanagh TA, Bevan MW (1987) GUS fusions: beta-glucuronidase as a sensitive and versatile gene fusion marker in higher plants. EMBO J **6:** 3901–3907

Jelitto-Van Dooren EPWM, Vidal S, Denecke J (1999) Anticipating endoplasmic reticulum stress: a novel early response before pathogenesis-related gene induction. Plant Cell **11:** 1935–1944

Jin H, Li S, Villegas A Jr (2006) Down-regulation of the 26S proteasome subunit RPN9 inhibits viral systemic transport and alters plant vascular development. Plant Physiol **142:** 651–661

Ju HJ, Brown JE, Ye CM, Verchot-Lubicz J (2007) Mutations in the central domain of potato virus X TGBp2 eliminate granular vesicles and virus cell-to-cell trafficking. J Virol **81:** 1899–1911

Ju HJ, Samuels TD, Wang YS, Blancaflor E, Payton M, Mitra R, Krishnamurthy K, Nelson RS, Verchot-Lubicz J (2005) The potato virus X TGBp2 movement protein associates with endoplasmic reticulum-derived vesicles during virus infection. Plant Physiol **138:** 1877–1895

Ju HJ, Ye CM, Verchot-Lubicz J (2008) Mutational analysis of PVX TGBp3 links subcellular accumulation and protein turnover. Virology **375:** 103–117

Kirst ME, Meyer DJ, Gibbon BC, Jung R, Boston RS (2005) Identification and characterization of endoplasmic reticulum-associated degradation proteins differentially affected by endoplasmic reticulum stress. Plant Physiol **138:** 218–231

Koizumi N, Martinez IM, Kimata Y, Kohno K, Sano H, Chrispeels MJ (2001) Molecular characterization of two Arabidopsis Ire1 homologs, endoplasmic reticulum-located transmembrane protein kinases. Plant Physiol **127:** 949–962

Krishnamurthy K, Heppler M, Mitra R, Blancaflor E, Payton M, Nelson RS, Verchot-Lubicz J (2003) The Potato virus X TGBp3 protein associates with the ER network for virus cell-to-cell movement. Virology **309:** 135–151

Leborgne-Castel N, Jelitto-Van Dooren EP, Crofts AJ, Denecke J (1999) Overexpression of BiP in tobacco alleviates endoplasmic reticulum stress. Plant Cell **11:** 459–470

Lee LY, Fang MJ, Kuang LY, Gelvin SB (2008) Vectors for multi-color bimolecular fluorescence complementation to investigate protein-protein interactions in living plant cells. Plant Methods **4:** 24

Liu Y, Burch-Smith T, Schiff M, Feng S, Dinesh-Kumar SP (2004) Molecular chaperone Hsp90 associates with resistance protein N and its signaling proteins SGT1 and Rar1 to modulate an innate immune response in plants. J Biol Chem **279:** 2101–2108

Liu Y, Schiff M, Serino G, Deng XW, Dinesh-Kumar SP (2002) Role of SCF ubiquitin-ligase and the COP9 signalosome in the *N* gene-mediated resistance response to *Tobacco mosaic virus*. Plant Cell **14:** 1483–1496

Lu DP, Christopher DA (2008) Endoplasmic reticulum stress activates the expression of a sub-group of protein disulfide isomerase genes and AtbZIP60 modulates the response in Arabidopsis thaliana. Mol Genet Genomics **280:** 199–210

Mahalingam R, Jambunathan N, Gunjan SK, Faustin E, Weng H, Ayoubi P (2006) Analysis of oxidative signalling induced by ozone in Arabidopsis thaliana. Plant Cell Environ **29:** 1357–1371

Malim MH, Emerman M (2008) HIV-1 accessory proteins: ensuring viral survival in a hostile environment. Cell Host Microbe **3:** 388–398

Martínez IM, Chrispeels MJ (2003) Genomic analysis of the unfolded protein response in *Arabidopsis* shows its connection to important cellular processes. Plant Cell **15:** 561–576

Medigeshi GR, Lancaster AM, Hirsch AJ, Briese T, Lipkin WI, Defilippis V, Früh K, Mason PW, Nikolich-Zugich J, Nelson JA (2007) West Nile virus infection activates the unfolded protein response, leading to CHOP induction and apoptosis. J Virol **81:** 10849–10860

Mekuria T, Bamunusinghe D, Payton M, Verchot-Lubicz J (2008) Phloem unloading of potato virus X movement proteins is regulated by virus and host factors. Mol Plant Microbe Interact **21:** 1106–1117

Mitra R, Krishnamurthy K, Blancaflor E, Payton M, Nelson RS, Verchot-Lubicz J (2003) The potato virus X TGBp2 protein association with the endoplasmic reticulum plays a role in but is not sufficient for viral cell-to-cell movement. Virology **312:** 35–48

Murai-Takebe R, Noguchi T, Ogura T, Mikami T, Yanagi K, Inagaki K, Ohnishi H, Matozaki T, Kasuga M (2004) Ubiquitination-mediated regulation of biosynthesis of the adhesion receptor SHPS-1 in response to endoplasmic reticulum stress. J Biol Chem **279:** 11616–11625

Navazio L, Mariani P, Sanders D (2001) Mobilization of Ca^{2+} by cyclic

ADP-ribose from the endoplasmic reticulum of cauliflower florets. Plant Physiol **125:** 2129–2138

Nomaguchi M, Fujita M, Adachi A (2008) Role of HIV-1 Vpu protein for virus spread and pathogenesis. Microbes Infect **10:** 960–967

Oh DH, Kwon CS, Sano H, Chung WI, Koizumi N (2003) Conservation between animals and plants of the cis-acting element involved in the unfolded protein response. Biochem Biophys Res Commun **301:** 225–230

Pazhouhandeh M, Dieterle M, Marrocco K, Lechner E, Berry B, Brault V, Hemmer O, Kretsch T, Richards KE, Genschik P, et al (2006) F-box-like domain in the polerovirus protein P0 is required for silencing suppressor function. Proc Natl Acad Sci USA **103:** 1994–1999

Petroski MD, Deshaies RJ (2005) Function and regulation of cullin-RING ubiquitin ligases. Nat Rev Mol Cell Biol **6:** 9–20

Preston AM, Gurisik E, Bartley C, Laybutt DR, Biden TJ (2009) Reduced endoplasmic reticulum (ER)-to-Golgi protein trafficking contributes to ER stress in lipotoxic mouse beta cells by promoting protein overload. Diabetologia **52:** 2369–2373

Qi Y, Zhong X, Itaya A, Ding B (2004) Dissecting RNA silencing in protoplasts uncovers novel effects of viral suppressors on the silencing pathway at the cellular level. Nucleic Acids Res **32:** e179

Ratcliff F, Martin-Hernandez AM, Baulcombe DC (2001) Technical Advance. Tobacco rattle virus as a vector for analysis of gene function by silencing. Plant J **25:** 237–245

Ren C, Pan J, Peng W, Genschik P, Hobbie L, Hellmann H, Estelle M, Gao B, Peng J, Sun C, et al (2005) Point mutations in Arabidopsis Cullin1 reveal its essential role in jasmonate response. Plant J **42:** 514–524

Sambrook J, Fritsch EF, Maniatis T (1989) Molecular Cloning: A Laboratory Manual, Ed 2. Cold Spring Harbor Laboratory Press, Cold Spring Harbor, NY

Samuels TD, Ye C-M, Ju H-J, Motes CM, Blancaflor EB, Verchot-Lubicz J (2007) Potato virus X TGBp1 protein accumulates independently of TGBp2 and TGBp3 to promote virus cell-to-cell movement. Virology **367:** 375–389

Schepetilnikov MV, Manske U, Solovyev AG, Zamyatnin AA Jr, Schiemann J, Morozov SY (2005) The hydrophobic segment of Potato virus X TGBp3 is a major determinant of the protein intracellular trafficking. J Gen Virol **86:** 2379–2391

Schott A, Ravaud S, Keller S, Radzimanowski J, Viotti C, Hillmer S, Sinning I, Strahl S (2010) Arabidopsis stromal-derived factor2 (SDF2) is a crucial target of the unfolded protein response in the endoplasmic reticulum. J Biol Chem **285:** 18113–18121

Schubert U, Antón LC, Bacík I, Cox JH, Bour S, Bennink JR, Orlowski M, Strebel K, Yewdell JW (1998) CD4 glycoprotein degradation induced by human immunodeficiency virus type 1 Vpu protein requires the function of proteasomes and the ubiquitin-conjugating pathway. J Virol **72:** 2280–2288

Seo PJ, Kim SG, Park CM (2008) Membrane-bound transcription factors in plants. Trends Plant Sci **13:** 550–556

Shadwick FS, Doran PM (2007) Propagation of plant viruses in hairy root cultures: a potential method for in vitro production of epitope vaccines and foreign proteins. Biotechnol Bioeng **96:** 570–583

Silva AT, Nguyen A, Ye C, Verchot J, Moon JH (2010) Conjugated polymer nanoparticles for effective siRNA delivery to tobacco BY-2 protoplasts. BMC Plant Biol **10:** 291

Slepak TI, Tang M, Slepak VZ, Lai K (2007) Involvement of endoplasmic reticulum stress in a novel classic galactosemia model. Mol Genet Metab **92:** 78–87

Surjit M, Jameel S, Lal SK (2007) Cytoplasmic localization of the ORF2 protein of hepatitis E virus is dependent on its ability to undergo retrotranslocation from the endoplasmic reticulum. J Virol **81:** 3339–3345

Surjit M, Lal SK (2008) The ORF2 glycoprotein of hepatitis E virus retrotranslocate from the endoplasmic reticulum to the cytoplasm and down-regulates NF-kappa B activity in human hepatoma cells. Infect Genet Evol **8:** S13

Tardif KD, Mori K, Kaufman RJ, Siddiqui A (2004) Hepatitis C virus suppresses the IRE1-XBP1 pathway of the unfolded protein response. J Biol Chem **279:** 17158–17164

Tateda C, Ozaki R, Onodera Y, Takahashi Y, Yamaguchi K, Berberich T, Koizumi N, Kusano T (2008) NtbZIP60, an endoplasmic reticulum-localized transcription factor, plays a role in the defense response against bacterial pathogens in Nicotiana tabacum. J Plant Res **121:** 603–611

Tzfira T, Vaidya M, Citovsky V (2004) Involvement of targeted proteolysis in plant genetic transformation by Agrobacterium. Nature **431:** 87–92

Urade R (2007) Cellular response to unfolded proteins in the endoplasmic reticulum of plants. FEBS J **274:** 1152–1171

Urade R (2009) The endoplasmic reticulum stress signaling pathways in plants. Biofactors **35:** 326–331

Urano F, Wang X, Bertolotti A, Zhang Y, Chung P, Harding HP, Ron D (2000) Coupling of stress in the ER to activation of JNK protein kinases by transmembrane protein kinase IRE1. Science **287:** 664–666

Verchot-Lubicz J, Torrance L, Solovyev AG, Morozov SY, Jackson AO, Gilmer D (2010) Varied movement strategies employed by triple gene block-encoding viruses. Mol Plant Microbe Interact **23:** 1231–1247

Wang XH, Aliyari R, Li WX, Li HW, Kim K, Carthew R, Atkinson P, Ding SW (2006) RNA interference directs innate immunity against viruses in adult Drosophila. Science **312:** 452–454

Whitham SA, Quan S, Chang HS, Cooper B, Estes B, Zhu T, Wang X, Hou YM (2003) Diverse RNA viruses elicit the expression of common sets of genes in susceptible Arabidopsis thaliana plants. Plant J **33:** 271–283

Williams B, Kabbage M, Britt R, Dickman MB (2010) AtBAG7, an Arabidopsis Bcl-2-associated athanogene, resides in the endoplasmic reticulum and is involved in the unfolded protein response. Proc Natl Acad Sci USA **107:** 6088–6093

Williams BL, Lipkin WI (2006) Endoplasmic reticulum stress and neurodegeneration in rats neonatally infected with borna disease virus. J Virol **80:** 8613–8626

Xu C, Bailly-Maitre B, Reed JC (2005) Endoplasmic reticulum stress: cell life and death decisions. J Clin Invest **115:** 2656–2664

Xu L, Liu F, Lechner E, Genschik P, Crosby WL, Ma H, Peng W, Huang D, Xie D (2002) The SCF(COI1) ubiquitin-ligase complexes are required for jasmonate response in *Arabidopsis*. Plant Cell **14:** 1919–1935

Yu CY, Hsu YW, Liao CL, Lin YL (2006) Flavivirus infection activates the XBP1 pathway of the unfolded protein response to cope with endoplasmic reticulum stress. J Virol **80:** 11868–11880

Zaltsman A, Krichevsky A, Loyter A, Citovsky V (2010) Agrobacterium induces expression of a host F-box protein required for tumorigenicity. Cell Host Microbe **7:** 197–209

Zamyatnin AA Jr, Solovyev AG, Bozhkov PV, Valkonen JP, Morozov SY, Savenkov EI (2006) Assessment of the integral membrane protein topology in living cells. Plant J **46:** 145–154

Zamyatnin AA Jr, Solovyev AG, Sablina AA, Agranovsky AA, Katul L, Vetten HJ, Schiemann J, Hinkkanen AE, Lehto K, Morozov SY (2002) Dual-colour imaging of membrane protein targeting directed by poa semilatent virus movement protein TGBp3 in plant and mammalian cells. J Gen Virol **83:** 651–662

Zhang K, Kaufman RJ (2006) The unfolded protein response: a stress signaling pathway critical for health and disease. Neurology (Suppl 1) **66:** S102–S109